

CapstanCrunch: A Haptic VR Controller with User-supplied Force Feedback

Mike Sinclair
sinclair@microsoft.com

Eyal Ofek
eyalofek@microsoft.com

Mar Gonzalez-Franco
margon@microsoft.com

Christian Holz
cholz@microsoft.com

Microsoft Research
Redmond, WA, USA

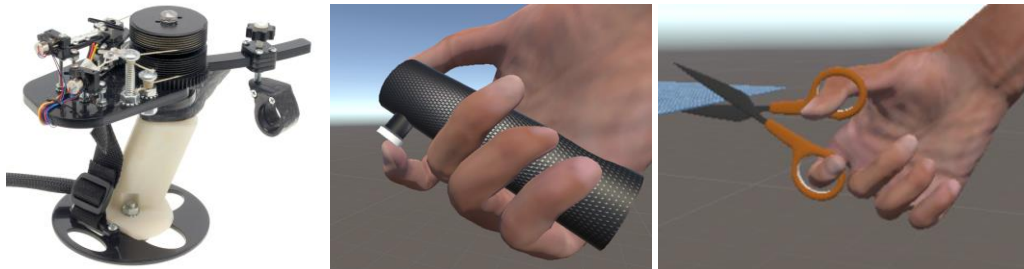


Figure 1: CapstanCrunch is a haptic controller that renders touch and grasp haptic sensations in virtual reality. CapstanCrunch supports human-scale forces during touch and grasp and can resist the user’s grasp force up to 20N. The friction-based capstan brake mechanism magnifies the small motor’s force, resulting in an integrated, palm-grounded controller design for interaction. The controller can render complex haptic events exhibiting variable stiffness and compliance.

ABSTRACT

We introduce CapstanCrunch, a force resisting, palm-grounded haptic controller that renders haptic feedback for touching and grasping both rigid and compliant objects in a VR environment. In contrast to previous controllers, CapstanCrunch renders human-scale forces without the use of large, high force, electrically power consumptive and expensive actuators. Instead, CapstanCrunch integrates a friction-based capstan-plus-cord variable-resistance brake mechanism that is dynamically controlled by a small internal motor. The capstan mechanism magnifies the motor’s force by a factor of around 40 as an output resistive force. Compared to active force control devices, it is low cost, low electrical power, robust, safe, fast and quiet, while providing high force control to user interaction. We describe the design and implementation of CapstanCrunch and demonstrate its use in a series of VR scenarios. Finally, we evaluate the performance of CapstanCrunch in two user studies and compare our controller with an active haptic controller with the ability

to simulate different levels of convincing object rigidity and/or compliance.

Author Keywords

Haptics; virtual reality, resistive force; brake capstan.

CCS Concepts

Hardware – Haptic devices

INTRODUCTION

In real life, we use our hands to interact with objects. We reach out for objects to touch, grasp, manipulate, and release them. In virtual reality (VR) however, such fine-grained interaction with virtual objects is generally not possible today. Commercially available VR controllers that are commonly used for interaction lack the ability to render realistic haptic feedback and support such natural use [8].

Research on haptic controllers in the context of realistic interaction in VR has recently become popular and produced a variety of prototypes that compete with the haptic rendering capabilities of gloves [11,26,31]. To provide more natural haptic experiences when interacting with virtual objects, individual controllers have been designed to render feedback in response to touching [7,17,41], dragging [14,37,48], single-handed grasping [15–17] and bi-manual grabbing [43,45]. All of these controllers contain intricate mechanisms to produce reasonable fidelity haptic sensations.

The main constraint to successfully render haptics for virtual objects in a realistic way is that a controller must be built to produce and endure human-scale forces during interaction and persist in rendering feedback, especially while grasping and squeezing objects when the force on the controller is highest. Achieving such magnitude of forces on handheld

Please do not modify this text block until you receive explicit instructions.

Permission to make digital or hard copies of all or part of this work for personal or classroom use is granted without fee provided that copies are not made or distributed for profit or commercial advantage and that copies bear this notice and the full citation on the first page. Copyrights for components of this work owned by others than the author(s) must be honored. Abstracting with credit is permitted. To copy otherwise, or republish, to post on servers or to redistribute to lists, requires prior specific permission and/or a fee. Request permissions from Permissions@acm.org. CONF '22, Jan 1 - Dec 31 2022, Authorberg.

Copyright is held by the owner/author(s). Publication rights licensed to ACM. ACM 978-1-xxxx-yyyy-zz/zz...\$zz.00. unique doi string will go here

controllers is challenging, especially since such devices are not earth-grounded.

Researchers have introduced a variety of controllers that produce strong grasping feedback. One solution is using an active mechanism with a strong servo motor (e.g., CLAW [17]), which results in a heavy, expensive, non-robust and power hungry design. An alternative is resisting the user applied force with a brake and stopping input movement at programmable points (e.g., Wolverine [16], Grability [15]), which can sustain high forces, but locks in the grasp at a certain point and requires manual release. This on-off lock is good for grasping rigid objects, but falls behind for rendering compliant objects, or rigid objects that require a computer-controlled release (e.g., crushing a can or an egg).

In this paper, we present a linear brake controller that can sustain human-scale forces [16]: CapstanCrunch (Figure 1), a haptic feedback device that uses a controlled brake technology to render grasp feedback at varying stiffness and/or compliance levels, and can sustain forces up to 20N. Resistive devices for haptics have advantages over active direct motor haptics in areas of stability, safety, power requirements, complexity, latency, force per device weight and cost. Our controller uses a capstan-based brake to produce variable pure resistive forces much like a unidirectional particle brake and a clutch-able spring that is capable of outputting the stored energy of a built-in spring for the perception of compliance. The capstan also exhibits a highly asymmetric behavior, resulting in an automatic and quick response in the release direction. This duality of a capstan brake and clutched spring creates a unique device that goes beyond the limitations of a binary brake and/or spring and can also resist human-scale forces.

In our evaluation, we compare CapstanCrunch against a real fixed-spring device and an active CLAW device to discover the performance limitations and explore the theory of asymmetric grip vs. release simulation. We also test all devices for midair pinch simulation and hyper-compliance.

Contributions

We introduce the following contributions in this paper:

- a modified capstan system used as a unidirectional linear brake,
- a variable-stiffness spring mechanism using the same capstan-based brake approach to render elasticity in haptic feedback,
- a low-cost, low-latency, cheap and simple twisted-string actuator whose low force is magnified by our mechanism,
- the validation of the device on a wide range of compliances and the comparison with other active or passive spring devices.

RELATED WORK

The work in this paper draws on related efforts of haptic controllers, human-scale forces, and grasp-based input. Haptic devices in the literature take either a stationary or a mobile

approach. The former are typically statically grounded to the earth in the user's environment and thus offer only limited reach, while the latter are worn or handheld and thus ungrounded.

Perception of Grasp

It is not surprising that previous research has focused on simulating forces for realistic grasping of objects. Many of the actions that the user will perform with a particular object will be determined by its compliance and/or weight [2].

In that regard, in the same way that existing models of grasp [19] explain how expectations of different object shapes will change how the hand approaches a grasp, users will also adapt their expectations and grasp after the initial interaction with the object. In essence, the main characteristics of the object will be derived from the initial interaction, and these will set the expectations for the rest of the manipulation, even for future release [9,24].

This perceptually driven grasp behavior can have very practical consequences for brake-type asymmetric devices, if only they were able to have non-binary braking. More precisely, if devices absorbing applied forces with brakes would also be able to render different spring constants for compliant objects, even if only in one direction – i.e. the grip part of the grasp could have high fidelity but the release follows a constant behavior – they could potentially still achieve a highly realistic performance because the release would be heavily influenced by the previous experience of the grasp.

Grounded Haptic Feedback

Due to the solid mounting to the environment, grounded haptic devices have the potential to provide haptic feedback at extreme forces, matching the user's input force and stopping their motion in place. Examples of grounded force-feedback devices include the Novint Falcon [21], PHANTOM [33], HIRO [20], or SPIDAR [35].

Such grounded feedback devices trade off force and spatial referencing with the possible reach during operation, as they limit user interaction to the area within reach. While larger-scale actuators can exceed human size (e.g., those used in assembly and fabrication) and produce even larger forces, their cost and need for installation becomes unrealistic for the use in interactive VR applications. An alternative is the use of passive haptic feedback that is statically grounded while redirecting the user's input to match the affordances of the static object (e.g., [13]).

Although not grounded to the environment, Canetroller is a tactile feedback controller that sustains human-scale forces while exploring the virtual environment for objects using the cane [50]. Canetroller is grounded to the user's hip using a combination of wearable straps that tightly couple the controller's magnetic particle brake to the user and enables Canetroller to brake the user's motions with the cane.

Ungrounded Haptic Feedback

Ungrounded devices are capable of being moved around and grounds the applied force input to the user's own body. In

the case of wearable interfaces, gloves and exoskeletons are usually grounded to the wearer's wrist or arm while handheld controllers are typically palm grounded.

Wearable Haptic Feedback

The most basic wearable haptic devices are finger-mounted actuators that render touch and pin-based texture [12] and shear [38] effects onto the user's fingertip. These effects can also be used to render the contact when grasping an object and simulate the object's gravity by deforming the finger pad [34], though they cannot produce force feedback.

These haptic devices typically come in the form of gloves or exoskeletons that either fully or partially cover the user's hand. To produce credible haptic sensations to the hand, such gloves and exoskeletons are often custom-fit, require careful putting on, and mount their mechanics along the outside of the wearer's fingers. Due to their coverage, they can render touch [26,30,31] and grasp [10,16,26,30,52] effects during interaction, simulating convincing haptic sensations.

Several implementation methods exist to implement such wearable interfaces. Resembling the human body, tendons [31], flexible metal strips [52], or finger phalanx replicas [26] along the outside of the hand allow room for interaction and grasping while rendering feedback. Others employ an in-hand design, thus grounded within the user's palm and matching each finger with an actuator [11] or in the form of a mitten [40,51] and can produce variable-stiffness sensations during grasping. Likely closest to the force feedback rendered by CapstanCrunch are Wolverine [16] and Gravity [15], hand-worn exoskeletons that use rails along which finger holsters slide during grasp interaction. Similar to CapstanCrunch, these holsters can be locked in place using small actuators, thereby effectively braking the user's grasp and stopping it while sustaining high grasp forces. Unlike CapstanCrunch, however, the user must release the applied force for these brakes to unlock, while our controller can gradually adjust the stiffness and/or compliance of force feedback at any time.

While the haptic sensations produced by haptic gloves and exoskeletons can be of high fidelity, their overhead for use is an unnatural weight and embodiment around the wearer's hand, the need for a careful mounting procedure, and the delicate mechanical elements and actuators that make their construction complex and expensive.

Haptic Feedback through Handheld Controllers

More recently and closely related to CapstanCrunch, numerous haptic prototype controllers have been researched that render more expressive haptic sensations than the vibrotactile effects found in most current commercial controllers [8,23]. In contrast to gloves and exoskeletons, controllers are easy to pick up and place down, they bear a handle that affords grabbing and holding them throughout interaction, and they can host haptic elements to render rich effects.

Exceeding the tactile sensations of vibrotactile motors, researchers have instrumented controllers to render kinesthetic

effects to simulate holding virtual objects. Depending on object interaction, controllers have moved internal weights to physically shift the center of gravity for the controller [44,49]. A similar effect has been demonstrated by oscillating multiple internal elements at different rates to create the impression of varying weight [4]. Even more, a series of controllers have produced the sensation of an external force acting upon them, for example using external gimbals [36,47] or air moving propellers [27].

Another class of haptic controllers produces tactile and kinesthetic effects on the user's finger while holding and moving the controllers around. While interacting with virtual objects, controllers can spin wheels under the finger to render shear forces [32] alongside varying materials [48]. Other controllers accommodate to the surface normals of virtual objects to give the user a sense of touching virtual shapes using a tilt and extrusion platform (NormalTouch [7]). By rendering such a tilt and extrusion "platform" using an array of texels, TextureTouch can render object textures in addition to surface orientations onto the user's fingertip while moving the controller around to explore objects [7].

Finally, several haptic controllers were designed to support grasping in VR, one of the most common activities after touch input [19]. TORC is a rigid controller that simulate grasps by individually vibrating the finger-pad surfaces when applying pressure during grasping [28]. CLAW is a haptic controller with a movable arm that can guide the user's finger to produce touch feedback, grasp force feedback, and object textures through vibration under the user's finger [17]. CLAW can also simulate compliant virtual objects and springs and force-open the user's grasp with considerable force. This is enabled by a strong servo motor that controls the controller opening, but comes at the cost of weight, power usage, some safety problems and size and cost of the actuator. Larger actuators are inherently capable of producing stronger force sensations, such as Haptic Links [43], which connect and dynamically brake to lock two controllers to support bimanual tasks, but increase weight, unwieldiness, and give up on the integrated form factors all controllers aspire to.

With CapstanCrunch, we provide strong force feedback sensations in an integrated form factor, reaping the benefits of controller use in VR while supporting the human-scale forces with dynamic compliance without the use of heavy and costly actuators. Our controller accomplishes this using a capstan-based friction brake mechanism whose resistance is controlled using a small motor ().

CAPSTANCRUNCH DESIGN AND IMPLEMENTATION

CapstanCrunch employs the resistive friction of a programmable brake for resisting human finger movements. We chose this method as it can be low-cost to implement, simple, safe, operate at human-scale forces, low latency, high speed and low electrical power requirement.

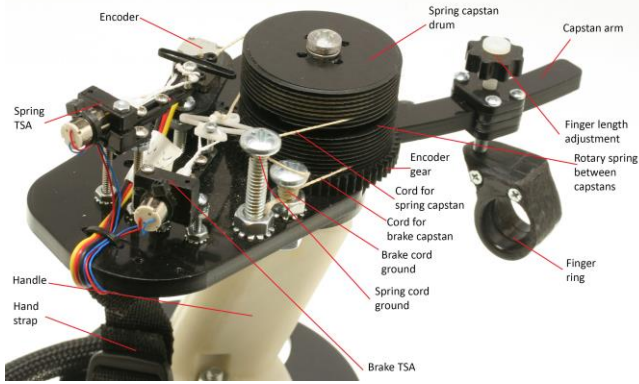


Figure 2: CapstanCrunch haptic controller.

We exploited the capabilities of a capstan brake, which enjoys the logarithmic force relationship of a drum wound with a cord. Figure 3 shows this relationship where cord-drum friction depends on the fixed total wind angle, tension on cord and fixed mutual friction coefficient between cord and capstan drum.

$$T_{load} = T_{hold} e^{\mu\phi}$$

where

- μ = friction coefficient between rope and capstan (unitless)
- ϕ = total rope wind angle around capstan

Note: $T_{load} > T_{hold}$

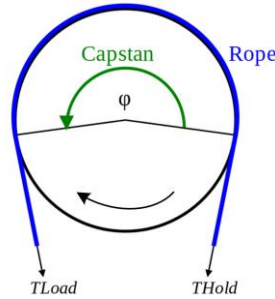


Figure 3: Basic capstan equation and cord relationship.: Basic capstan equation and cord relationship.

Note that like most capstan systems, the friction relationship between cord and drum is either static (non-moving capstan with regard to the cord) or dynamic (capstan rotating). Because we could not find data for the mutual static and dynamic friction coefficients, we have empirically tested many capstan-cord friction relationship pairs to discover one that has a minimum difference and hysteresis between static and dynamic friction (small stick-slip coefficient), so that we may be able to operate the brake in a linear fashion and not just in binary on/off mode.

During our exploration, we discovered that pairing acetal (e.g., Delrin) for the drum material with Vectran (an LCD plastic from Celanese Corporation) allows us to operate the brake in a nearly-linear fashion. Besides being slippery on acetal, Vectran has a high tensile strength, stretch resistance and low creep.

CapstanCrunch Controller

The final CapstanCrunch prototype is shown in Figure 2. The photo shows the two cascaded capstan drums wound with Vectran cord, grounded to the device frame on one side of the drum and actuator-connected on the other. What is not visible is the rotational spring connecting the two capstan drums to produce the programmable compliance haptic. The

fixed static thumb rest of the controller is occluded in this photo.

Throughout development, all of our controller prototypes had 6DOF Vive trackers attached during use which located our controllers in 6DOF space and could thus infer the location of the user's finger and thumb in the VR scene to articulate a virtual hand with inverse kinematics [42].

Figure 4 shows the mechanical components and connections of CapstanCrunch. Note the brake and/or spring devices can programmatically exhibit resistive forces on the finger.

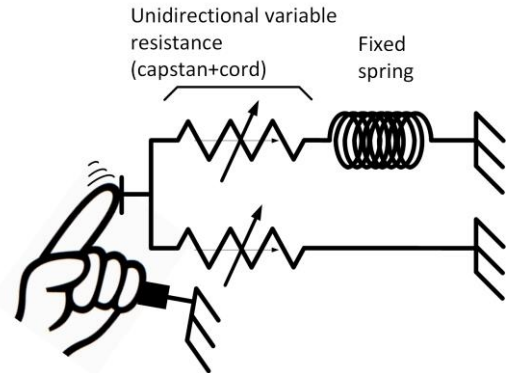
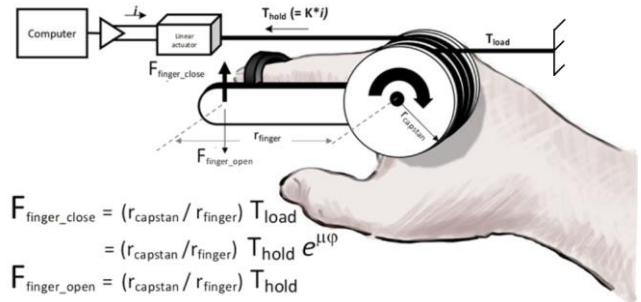


Figure 4 CapstanCrunch mechanical diagram

Linear Brake Engagement and Release

Unlike most capstan systems where the cord moves with reference to the drum, the capstan drum in our controller is rotated by the user's finger and the cord is fixed. shows a schematic of the brake system and lists the equations of force. A small internal actuator applies a low-tension force (T_{hold}) on a cord where the higher tension (T_{Load}) side of the cord is fixed (grounded) to the handheld device. Thus, when the user tries to rotate the capstan in a counterclockwise direction (finger closing) with small or no T_{hold} actuator tension, the capstan drum rotates more or less freely with no opposing force. As the T_{hold} tension is increased by the actuator, T_{Load} increases exponentially, making the drum harder to turn in the counterclockwise direction.



$$F_{finger_close} = (r_{capstan} / r_{finger}) T_{load}$$

$$= (r_{capstan} / r_{finger}) T_{hold} e^{\mu\phi}$$

$$F_{finger_open} = (r_{capstan} / r_{finger}) T_{hold}$$

Figure 4: Schematic of our brake-only system showing finger force vs cord tension relationship.

When the user rotates the drum in clockwise direction, T_{hold} is automatically lessened by moving the cord exit point of the drum closer to the internal actuator. With T_{hold}

automatically releasing by reversing direction of the capstan (finger opening), we implement a highly asymmetric force device in CapstanCrunch, similar in operation to commercially available one-way brakes.

Using this method, the user experiences a programmed force as the finger closes and a very low force as the finger opens where no resistive force is desired.

In practice, however, there exists a sticking force of the cord to the drum after a strong closing force event, so that all tension is indeed not released when the user opens their finger. We believe this may be due to the weave of the Vectran cord, adding a small initial stretch and partially seating into the soft acetal. We overcome the sticking force by monitoring the finger position encoder. When it is evident that the user is moving their finger away from their thumb, the controller applies a small reverse pulse to the TSA actuator which further releases the low-side tension on the cord and thus releases the drum to rotate freely.

Firmware control loop

The code controlling the behavior of CapstanCrunch inputs the finger-position encoder as the sole input by converting the rotary potentiometer encoder output geared to the capstan drum to a voltage. Having this encoder as the only feedback element in our controller allows for a simple and low-cost implementation that requires no expensive force sensors. Based on the finger-position sensor sampled at 20 kHz by our control loop, CapstanCrunch adjusts its force feedback behavior and spring engagement by driving the respective actuator via a PWM signal that produces predictable and repeatable forces in resistance following the capstan equation.

A Teensy 3.6 microcontroller runs the firmware in our controller, converting and processing the rotary encoder signal directly to produce a PWM signals for the actuators. The PWM terminals of the microcontroller connect to a current limiting DRV6671 motor driver H-bridge, which drives an E-flite EFL9052 coreless motor.

The Teensy microcontroller is connected to a PC through a serial connection to specify compliance, spring, and brake settings from within our VR environment in the form of an event schedule. The schedule is a list of positions and forces at which the capstan should actuate given a finger position. Tracking the controller in 6D and depending on its position and orientation, we specify the finger opening angles at which CapstanCrunch should apply certain compliance or brake forces, which are then executed and output at 20 kHz within our control loop. CapstanCrunch responds to changes in opening angle and adjusts forces activations with negligible latency.

Rendering Haptic Effects

Having constructed this mechanism, we discovered many haptic events can be synthesized based on the programming resistive and compliant forces. When the finger encoder

reports the appropriate contact position with the object, the brake is actuated to the desired low-tension force, which is immediately mechanically communicated to the user's finger as a resistive force. For the simulation of squeezing something less hard than a rigid object, like clay for example, the actuator is commanded to actuate at a less force than in the previous example. The user feels the contact with the clay but, with enough applied force, is able to squeeze and deform it with the appropriate visuals appearing in the VR display.

Eliminating Cord Overlap

To correct for possible cord-overlap problems previously experienced, we machined a helix or thread-like groove in the acetal drum. Figure 5 shows the modified capstan drum that now traps the new cord in the deep grooves, such that it stays keeping it in place and will not overlap, but still interacts with the acetal surface correctly.



Figure 5: A helix groove machined into the acetal drum to prevent cord overlap.

Adding Compliance to the Haptic Brake

To add the haptic perception of compliance, we connect a second capstan to the brake capstan through a rotary or torsional spring. This second capstan acts as a clutch to engage the spring at the appropriate time. Figure 6 shows an exploded view of our assembly.

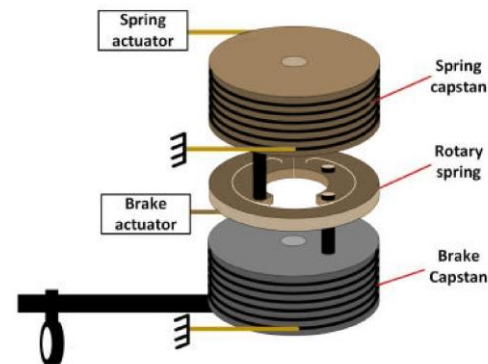


Figure 6: Exploded view of the rotational spring coupling the spring capstan to the brake capstan

This spring capstan also has its high-tension LOAD cord side grounded to the controller body and the low-tension HOLD side connected to a second low force actuator. With no actuation of the spring and brake capstans, they rotate freely with finger closing. If just the spring capstan is actuated at maximum force, the finger movement and brake capstan are connected through the rotary spring and capstan to ground. In this case, the user experiences squeezing a spring with a constant spring coefficient, k . Thus

$$\text{Finger_closing_force} = k * \text{Finger_closing_distance}$$

(from actuation position)

Note that k is a constant in this case. If we were to let the spring capstan slip due to a smaller actuation force and/or apply a small linear braking force, we can modulate the perceived spring constant k' that the user feels. The perceived compliance now is a function of the fixed spring constant, how much the spring capstan slips, and how much brake is applied. We can synthesize many different perceived spring behaviors by using these variables. See the user test section for how this is perceived.

Twisted String Actuator

Finally, to overcome the lower speed of motor+gears actuators, we exploit the technology of a Twisted String Actuator (TSA). This technology has been around for centuries and functions well in this application [22].

The TSA we built into CapstanCrunch shown in Figure 7 consists of a small pager motor with a hub attached that winds up a pair of strings (Spectra fishing line, 100 pound test) against a rotationally fixed but sliding arm. As the string is wound by the motor, it pulls on the sliding arm coupled to the small connection spring and applies cord tension to the HOLD side of the capstan as a function to current supplied to the motor.

The small connection spring serves as compliance added to the actuator to make up for the small apparent cord stretch as tension is increased and the capstan turns, changing the both HOLD and LOAD tensions by a small amount. This apparent cord stretch does not appear to agree with the manufacturer's stretch specifications of the cord, but, after checking with the manufacturer, is mainly due to the initial contraction of the cord's weave geometry plus bending of the cord around the drum.

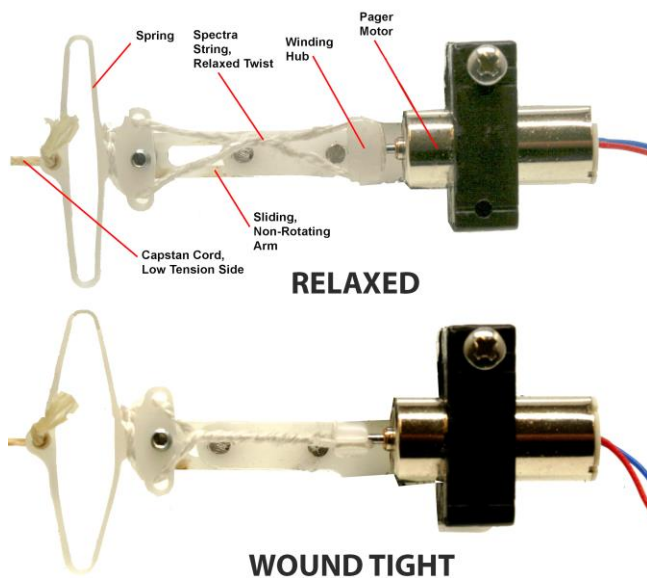


Figure 7: Twisted String Actuator (TSA) for supplying the capstan's low-tension LOAD input.

The TSA is also known for its efficiency in converting electrical to mechanical energy plus its back-drivability, which is better than with spur gears. Also, because of its energy conversion efficiency plus low inertia load and coreless motor design, the response and latency is much faster than the previous actuator or most hobby servo motors. The TSA also produces no noise as is characteristic of actuators with gears.

Early Prototypes

We created many early prototypes in the search for CapstanCrunch. In this section, we briefly present some of the challenges we found when creating CapstanCrunch. Figure 8 shows an annotated image of an early prototype we built to explore the capstan brake. While the user holds the handle in their palm, the index finger slips easily into the finger ring. As the user opens and closes their finger, the finger bar, encoder gear, and capstan drum rotate as one. Around the cylindrical capstan drum is wound the cord with the LOAD end terminated (grounded) to the frame and the HOLD end connected to the internal actuator.

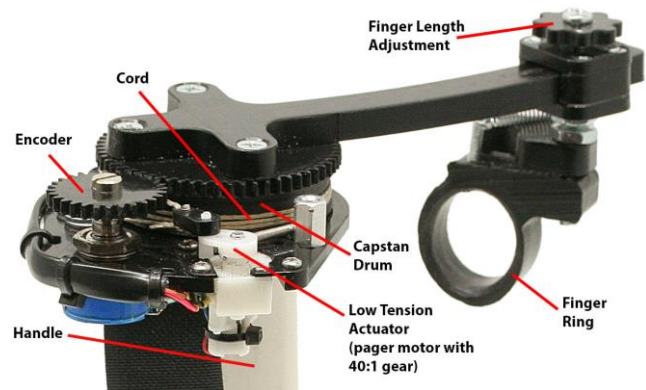


Figure 8: Early capstan-based friction brake design

The actuator in our early controller prototypes is a commercially available assembly of a pager motor with spur gears yielding a 40:1 gear ratio with a rotating lever as the output. This offers enough tension for the low-tension HOLD input to the capstan system while operating at around 140 ms from cord loose-to-tight.

There were problems with this particular implementation, however. Since there is no source of an active forcing device pushing on the user's finger or internal mechanical energy storage, there was no acceptable method of simulating a spring or other compliant haptics which we believe important. Also, there is the possibility of a cord "over-wrap" where the cord gets wrapped on the drum with one or more layers overlapping others. This destroys the predictability of friction and can cause permanent lock-up of the brake. Another problem exists with the slow actuation time of the internal actuator. At ~140 ms, it is hard to actuate the device at the correct time if the user's finger is moving too fast. Employing extrapolation as a firmware solution of prediction to brake at the right time did not result in a much-improved behavior during testing.

MECHANICAL PERFORMANCE TESTS

Multiple performance tests were carried out to create the final mechanical prototype. The performance was as follows:

- Stiffness achieved at max force: 5.88 N/mm
- Latency TSA driver signal to output force: 6.5ms
- Force dynamic range <math>< 0.2\text{N} \rightarrow 20\text{N}</math> (or $\sim 100:1$)

The force measurements were acquired using the setup in **Error! Reference source not found.** A computer controlled geared stepper motor moves the finger rest towards the thumb while the modified force transducer records the applied force and finger position at a 10KHz sampling rate.

Actuation Latency

We used a Fuji HS-10 with a 1000 fps function video camera to record and analyze the winding and unwinding response at maximum actuation speed. This measurement reported 5 ms for actuation and 5.2 ms for release. As for longevity, we programmed the actuator to cycle every second for 24 hours (86,400 cycles) with no appreciable deterioration in the string or motor behavior. After 3 days of continuous cycling however, the motor was harder to turn when winding. This was probably due to a wearing of the bearings in the motor, which were not designed for an axial load, only for radial loads. We believe a thrust bearing could be designed into the motor or system for longer wear. Figure 9 shows an automated system we designed to test our capstans and completed systems.

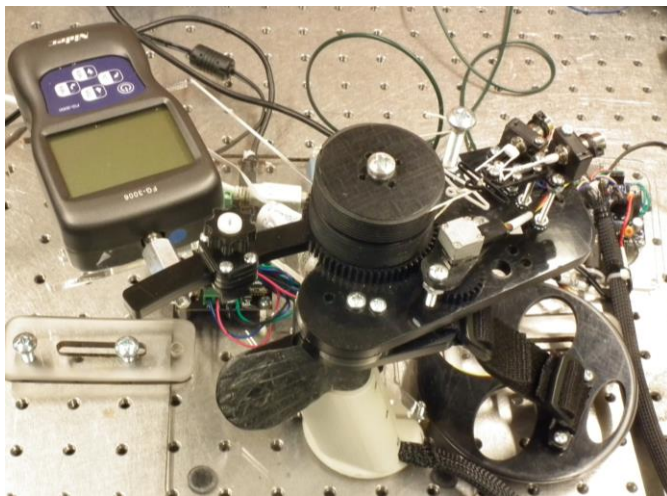


Figure 9: Robotic Force vs Finger-Thumb Distance Measurement Setup. A computer controlled geared stepper motor moves the finger rest towards the thumb while the modified force transducer records the applied force at a 10KHz sampling rate.

USER STUDY

A user study was designed to evaluate the performance of grasping with CapstanCrunch. Participants were presented with 6 virtual objects of different compliances (ranging from rigid to “thin air” in which no resistance should be expected). Each object was featured in 5 different sizes. Using this library of objects, we explored how well CapstanCrunch

performed as compared to a fixed spring system device (Figure 10 right) and an actuated controller that could actually deliver a symmetric grip and release simulation (CLAW, Figure 10 left). As per design, CapstanCrunch had an asymmetric rendering in which the grip spring constant can be modulated but the release will remain fixed.

We rendered objects visually according to their size and compliance along with synchronized haptic rendering using 3 different methods (physical spring, motorized CLAW and CC). Participants graded the haptic simulation compared to their expectations from the visual behavior, if the visual and haptic simulation fit their expectation, they would rate it high on the realism score.

Given the capstan + TSA nature of CapstanCrunch, the comparison to the spring device was intended to provide a baseline experience of a truly compliant grasp, and the CLAW provided a baseline of a complete rigid grasp that can brake on demand without friction.

Participants

We recruited participants from our institution through internal e-mail. In total, 12 participants (2 female, age from 27 to 51) completed the user studies. All participants were right-handed. All participants gave written informed consent according to the declaration of Helsinki and were paid \$15 for their participation. This user study was approved by an Institutional Review Board.



Figure 10: Left) Claw device. Right) Fixed-Spring device. The Spring device was built as a copycat of the other two prototypes CapstanCrunch and CLAW with the difference that the finger arm was only connected to a fixed spring.

Apparatus and Experimental Setup

Participants were equipped with an HTC Vive VR Headset, and one of three devices: CapstanCrunch, Spring, or CLAW. The CapstanCrunch was designed as described in previous sections, the CLAW was unmodified [17], and we constructed the Spring device as a close replica of the other two prototypes with the only difference that the finger arm was connected to a fixed spring (Figure 10). All devices were attached to a tracking system and a virtual hand was rendered in the position of the participant’s hand in the HMD (Figure 11).

Participants experienced the three devices in a blinded manner, i.e. they were given the devices after they were already wearing the HMD and did not have prior experience with the devices. The study followed a within-subject design in which

all participants used all devices in random orders following a Latin-square randomized permutation.

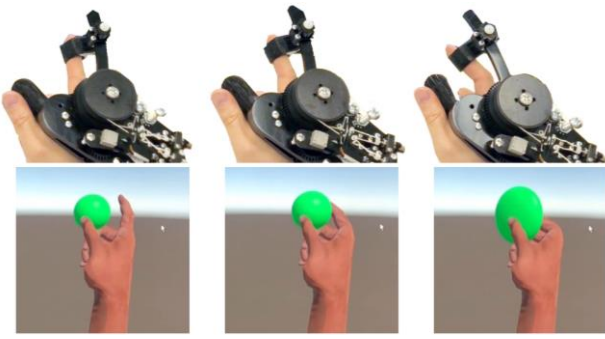


Figure 11: Example of a compliant ball grasp and release with CapstanCrunch during the user study.

The task was always the same: participants were given a virtual ball in hand and had 5 seconds to pinch it multiple times and thus experience the simulated compliance with the particular device. The main experiment consisted on a randomized sequence of balls with different stiffness and sizes (Figure 11).

In total participants completed $6 \times 5 + 1 = 31$ conditions (i.e., 6 balls, 5 sizes + 1 midair). After each ball participants rated from 1 to 7 how realistic they felt the touch+visual experience was. At the end of each device they were asked quantitatively what were the most and least liked aspects of the immediate experience they had with that particular device. The experiment lasted less than 30 minutes.

Stiffness Range

There was a total dynamic range of 7 stiffness levels, ranging from thin air pinch, to completely rigid balls. The middle point stiffness was presented in which the k constant of the spring for the CapstanCrunch, Spring and CLAW was equilibrated to 0.5 N/m. For the particular case of the Spring and CapstanCrunch that was matched their ground truth k . Because the CLAW is actuated via a motor, there was no actual ground truth k . Therefore, we defined Ground Truth, as the virtual object with compliance equal to the spring constant used by both the physical springs device as well as CC. For this object, ALL devices should render a “perfect” haptic feedback and should rank high by the users. When rendering objects of different compliance, the CC, CLAW, and the spring rendering will stray in fidelity from the expected physical response.

Two balls were of greater k than the ground truth and two were of smaller k . In order to simulate smaller k , we developed a retargeting technique in which the movements of the participants are amplified to make the ball look squeezier than the actual device [6]. The idea being to create illusions of hyper compliance, even when the springs are not able of delivering such small k , a sort of haptic retargeting for compliance [1,6,25]. By amplifying the movement effectively, we created an illusion of greater distance (d) and the mental Hook’s law equation of $F=k*d$ got distorted, creating the illusion of a smaller k . For the case of the Spring device we

also did a retargeting for the 2 balls with greater k , for which we did the opposite and scaled down the movements of the users to simulate larger k .

Size Range

Additionally, the different stiffness balls were presented with five different ball sizes (4cm, 5cm, 5.5cm, 6cm, 7cm). The size changes introduction was two folded: (i) to avoid easy recognition of the 6 different balls, (ii) to account for the importance of proprioceptive drifts during grasp on our compliance retargeting technique, but also when using the Spring device. In the case of the Spring device, the location at which the finger-arm would start engaging the spring was fixed, thus the virtual finger would be recalibrated to be always in touch with the ball at that precise instant (the ball that corresponded to a 1-to-1 size was the 5.5cm ball). Whereas with the other devices, that trick was not necessary as they could engage at the particular angle when the finger-arm entered in contact with the ball. The ground truth ball size was calibrated to match 1-to-1 the spring engagement point of the Spring device.

Results

Through our user study, we have compared the performance of CapstanCrunch to a fixed Spring grasping device and a CLAW prototype. Results show that CapstanCrunch significantly beats the results of a fixed Spring device in all comparisons minus ground truth.

We ran a repeated measures ANOVA on a Linear Mixed-Effects Model with 3 factors: Stiffness, Size and Condition. Significant effects were found for Condition ($F(1, 1084)=57.6, p<0.001$) and for the interaction Condition x Stiffness ($F(2, 1084)=134.76, p<0.001$). There were no effects nor interactions for the size of the balls.

Doing a complete aggregation of the performance scores for the different conditions (Figure 12), we found that there were significant differences in the scores across the devices (Friedman paired-test: $\chi^2(2)=12.8, p=0.001$). Post-hoc Conover tests were applied for further pairwise comparisons with Bonferroni correction. This analysis showed that CapstanCrunch (score $M=5.35, SD=0.8$) provided a significantly higher realistic haptic experience than CLAW ($M=4.79, SD=1.15, p=0.03$) and Spring device ($M=4.24, SD=1.21, p<0.001$). CLAW was also significantly better than the Spring device ($p<0.001$).

When looking more in detail, at ground truth compliance, the Spring device and the CapstanCrunch are equivalent as both render 1-to-1 the exact haptics and visuals to the user’s grasp. For all the rest of comparisons (from midair pinch to a rigid object), we found that the CapstanCrunch beats the Spring device, especially for more rigid objects, where the spring performs particularly bad.

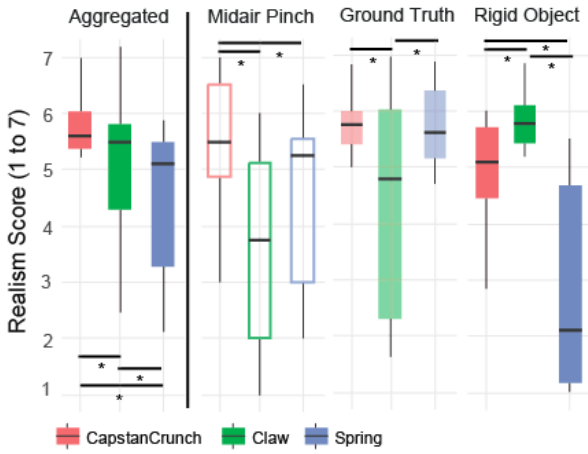


Figure 12: Device Preference. Tukey Boxplots showing the scores for realism of the device (mean score across all stiffness and sizes) and midair pinch as perceived by the participants. Significant differences with Friedman paired comparisons are marked with asterisk. The medians are the thick horizontal lines and the boxes show the interquartile ranges (IQR). The whiskers extend from lower quartile—1.5*IQR to min lower quartile + 1.5*IQR.

When compared to the CLAW, CapstanCrunch did not beat the levels of realistic rigidity accomplished by the CLAW. However, CapstanCrunch beat the CLAW for the Ground Truth in which the virtual visuals of the object rendered exactly the k of the TSA spring, and in general, was also a more preferred option for midair pinch (zero resistance) and hyper-compliant objects.

Stiffness Perception

We wanted to further understand the aggregated scores for haptic realism (i.e. how much did the visuals match the haptic simulation) of the different devices (Figure 13). To do so, we explored the performance for the different stiffness renderings (from hyper-compliant balls to rigid). We found that for the CLAW, there was a significant positive correlation between Stiffness and Score (Pearson’s correlation $r=0.5$, $t(82)=5.36$, $p<0.001$). On the contrary, the Spring device had a significant negative correlation between Stiffness and Score ($r=-0.38$, $t(82)=-3.7$, $p<0.001$) (Figure 13, Table 1).

| Realism Scores per Device (Mean ± Standard Deviation) | | | |
|--|---------------|-----------|-----------|
| Stiffness | CapstanCrunch | Claw | Spring |
| k/100 | 4.5 ± 1.5 | 3.6 ± 1.8 | 4.4 ± 1.6 |
| k/10 | 5.5 ± 0.8 | 4.5 ± 1.8 | 5.7 ± 1.2 |
| k | 5.7 ± 0.5 | 4.5 ± 1.8 | 5.6 ± 1.1 |
| k*20 | 5.5 ± 1.1 | 5.6 ± 0.9 | 3.8 ± 1.4 |
| k*200 | 5.3 ± 0.8 | 5.8 ± 0.9 | 3.0 ± 1.6 |
| Rigid | 4.9 ± 0.9 | 5.7 ± 0.7 | 2.8 ± 1.9 |

Table 1. Realism Scores (Mean and Standard Deviations) for the different stiffness levels and devices.

These results indicate that the renderings by the CLAW tended to become more realistic as the stiffness of the object

increased, while low stiffness levels in the CLAW were perceived worse. On the contrary the Spring device was particularly worse as the objects became stiffer and participants found it more realistic for bouncy objects.

These results indicate that the renderings by the CLAW tended to become more realistic as the stiffness of the object increased, while low stiffness levels in the CLAW k were perceived worse. On the contrary the Spring device was particularly worse as the objects became stiffer and participants found it more realistic for bouncy objects.

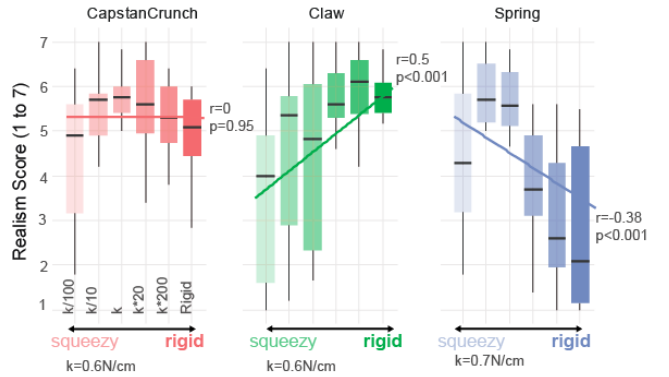


Figure 13: Realism scores for Stiffness levels across the three different devices in our evaluation

Using the same correlation analysis, we find that CapstanCrunch did not suffer such effects and the values of stiffness ($p=0.95$, $r=-0.006$), meaning that it had a higher dynamic range in the realism score across the different compliances.

In order to further investigate which device performed best for each of the stiffness levels we further analyze the within subjects effects for the rendering of Rigid Objects, the Ground Truth Objects (where the k of the device and that of the visuals matched), and the use of the controller in midair.

Midair

We asked participants to evaluate the perception of the devices when pinching in midair (Figure 12). Results show that participants scored significantly better the CapstanCrunch ($M=5.46$, $SD=1.25$) than the CLAW ($M=3.54$, $SD=1.72$) or the Spring device ($M=4.58$, $SD=1.64$) (Friedman paired-test: $\chi^2(2)=8.2$, $p=0.016$). Post-hoc Conover tests were applied for further pairwise comparisons with Bonferroni correction, this analysis showed that CapstanCrunch was significantly better for midair pinch than the Spring device and CLAW ($p<0.001$). While CLAW and Spring device were not significantly different ($p=0.33$). This is probably due to the fact that when unengaged CapstanCrunch offers zero resistance, and the same is not true for the other devices. CLAW requires always a motor engagement and the fix spring device will always give some compliance.

Rigid Object

We asked participants to evaluate the perception of the devices when the objects were completely rigid (Figure 12). Results show that the CLAW ($M=5.7$, $SD=0.7$) and

CapstanCrunch ($M=4.9$, $SD=0.9$) scored quite high for rigid objects, despite the CLAW was able to convey more realism ($p<0.001$). As expected, the Spring device ($M=2.8$, $SD=1.9$) performed significantly worse than the other two devices ($p<0.001$).

Compliant Ground Truth Object

We asked participants to evaluate the perception of the devices when the virtual object, the hand and the device were matched 1-to-1, i.e. the k constant of the spring in the device was matched by the virtual simulation. Results (Figure 12) show that participants scored significantly better the CapstanCrunch ($M=5.7$, $SD=0.5$) and the Spring device ($M=5.5$, $SD=1.0$) than the CLAW ($M=4.5$, $SD=1.8$) ($p<0.036$). While the Spring device and the CapstanCrunch were not significantly different ($p=1.0$).

The difference between the CLAW and the other devices could be due to the fact that there is no ground truth for CLAW, and we always relay on a simulation of a spring for this device, which in this case simulated a k constant similar to the Spring device and CapstanCrunch.

INTERACTION SCENARIOS IN VIRTUAL REALITY

Using CapstanCrunch, we can provide haptics for objects of variable complexity beyond the compliant balls explored in the user study in which springs and rigid interactions are not linear or get combined creating a more complex object.

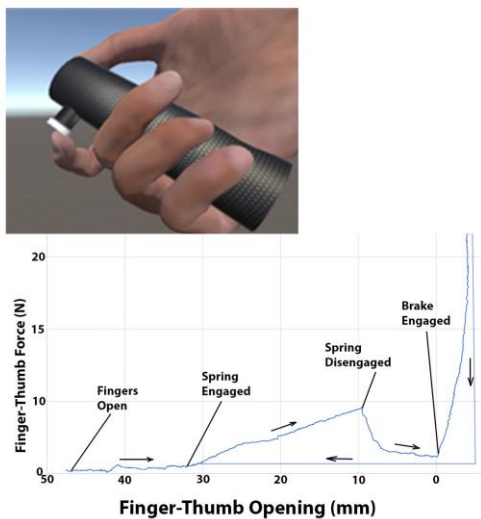


Figure 14: Forces and events applied by CapstanCrunch during the activation and release of a simulated button.

Examples of non-linear haptic grasp in which the forces and events applied during the interaction follow a complex sequence as determined by the forces and distances between fingers applied by the user, include the non-linear activation and release of a push button (Figure 14: Forces and events applied by CapstanCrunch during the activation and release of a simulated button.), the assembly of toy construction blocks (Figure 15), or the use of a pair of scissors (Figure 16: Forces and events applied by CapstanCrunch when the user operates scissors to cut. The gradual increase in length is

approximated by discrete steps. In this example, we chose 3 steps which gave a feeling of increasing difficulty to cut.).

In the case of the push button simulation (Figure 14: Forces and events applied by CapstanCrunch during the activation and release of a simulated button.), the user starts by a no-force movement toward the surface of the button which is a spring+brake combination. During closing of the finger towards the thumb, the user feels no force against the finger. When the user's finger touches the button, an added compliance is applied by the spring capstan. As the user pushes further, the spring acts alone until the finger reaches a point where the spring is released and the user feels no force for a short travel. Going further, the user encounters a full brake stop resistance and cannot push further. There is also a defined release path which is indicative of a typical button with a large hysteresis.

Another example of complex interaction that we implemented with CapstanCrunch was the assembly of toy construction blocks (Figure 15). When two blocks snap together, there is a hysteretic force loop experienced. In particular, there are three stages to the assembly. At first, the two block parts are separated and are brought together by pushing the finger ring in midair with no/low force. Stage 2, when the two pieces touch, the user feels the initial touch and the blocks completely mesh when enough force is applied. Once the blocks are assembled, the brake stops any further finger closing and the finger can retreat.

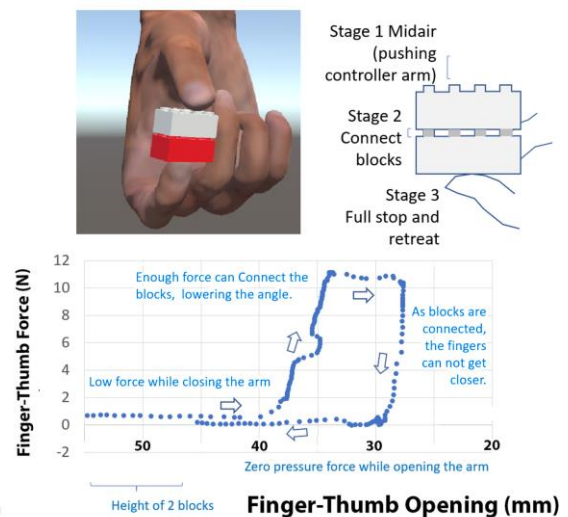


Figure 15: Forces and events applied by CapstanCrunch during the assembly of two building blocks.

In a final example of complex interaction, we implemented with CapstanCrunch, users can cut materials with a pair of scissors (Figure 16: Forces and events applied by CapstanCrunch when the user operates scissors to cut. The gradual increase in length is approximated by discrete steps. In this example, we chose 3 steps which gave a feeling of increasing difficulty to cut.). The gradual growth of the force

due to the increase of the material’s lever length is approximated by discrete steps.

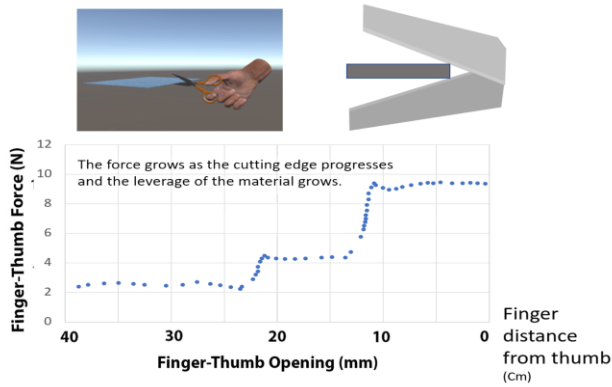


Figure 16: Forces and events applied by CapstanCrunch when the user operates scissors to cut. The gradual increase in length is approximated by discrete steps. In this example, we chose 3 steps which gave a feeling of increasing difficulty to cut.

We chose 3 steps, which gave a feeling of increase difficulty to cut as the scissors closed. Other complex object interactions that can be enabled with CapstanCrunch include the grasp of a glass that with enough force cracks into pieces. All forces were measured with a Nidec FG-3000 force gauge modified to record at >1000 Hz. For the axis “Finger distance from thumb” we simultaneously recorded the finger position encoder.

DISCUSSION

Performance Testing

When compared to other brake or capstan-based prototypes beyond CLAW, we found some remarkable aspects relevant both in design and performance.

CapstanCrunch was similar in some respects to Conti & Kahtib that used a modified SEA to simulate a safe bidirectional haptic rendering [18]. Their design was focused on a grounded device where both stiffness and elasticity were rendered together with the ability for force redirection in a multi-dimension system. While, CapstanCrunch was designed to be a hand-held format, which reduced the need of dimensionality. This way CapstanCrunch can achieve high performances in a smaller form factor, for example being hand-held we could focus on a 1D restrictive force only in one direction. In essence, both systems use a similar method, but CapstanCrunch differs from their H2O actuator, as a brake (maximum stiffness of 5880 N/m) is used instead of their motor. CapstanCrunch’s solution also increases our stiffness dynamic range over a SEA solution plus increases the energy efficiency but with a compromise in rendering fidelity of compliant objects.

Agarwal et al. [3] used a SEA also in their prototypes, but it was mainly used as a method to measure the applied output force in a motor-based closed loop system. CapstanCrunch instead employs a more energy efficient resistive brake

system plus a fixed spring and a brake as the user’s force sources. In that regard, an active system with force feedback, can simulate variable stiffness and elasticity with greater fidelity but with less efficiency.

In their tendon driven devices, Kang et al. used a capstan brake between a motor and the load in order to maintain tension in the cable when the motor is turned off [29]. Because CapstanCrunch is not envisioned as a tendon, it does not require output forces in both directions. The user only encounters a low (<0.2 N) force in the non-actuated (finger opening) direction.

In another tendon approach, Vigarù et al, employed servo motors and tendons for remotely actuating a haptics device [46]. However, motors were the main source of force in that design, where CapstanCrunch uses a brake.

In another motor-brake based systems, An et al. used a combination of a motor operated in closed loop and a brake for investigating a hybrid haptic actuator capable of simulating variable stiffness and elasticity as well as maintaining stability [5]. The main difference to CapstanCrunch is that it employs proportional brakes that are inherently stable and can programmatically administer a combination of stiff and/or (fixed) compliant output resistance forces. Other motor and brake designs such as Rossa et al. [39] used both a motor plus two bidirectional brakes to produce an output force simulating variable haptic elasticities. Though we believe this method more closely approaches any desired elasticity, our approach is a compromise for a compact hand-held controller that can achieve high performances on user tests.

User Testing

We have demonstrated the ability of CapstanCrunch to provide a high dynamic range of compliances (from midair no-force pinch to a compliant object to a rigid object). Additionally, we showcase a variety of complex interaction scenarios (using scissors, assembling toy blocks or pressing a button) that combine multiple stiffnesses and compliances in grasping events in which the intrinsic forces and rigidities can dynamically change.

The user study revealed a surprising new effect: users put more weight on grasping than releasing when it comes to perception of object compliance. We expected the full motorized CLAW to be chosen as the best experience, because CapstanCrunch changes haptic rendering only on the hand compression direction and uses a fixed spring in the other direction. Our device was therefore asymmetric, however, it showed high satisfaction levels of participants when compared to the CLAW. That can be explain by the fact that users draw higher attention for compressing the object vs. relaxing the grip (usually used to release the object from hold). This surprising behavior may impact on the design of haptic controllers in the future.

Through our user study, we have compared the performance of CapstanCrunch to a fixed Spring grasping device and a CLAW prototype. As expected, CapstanCrunch significantly

beats the results of a fixed spring device in all comparisons other than ground truth. At ground truth compliance, the Spring device and the CapstanCrunch are equivalent as both render 1-to-1 the exact haptics and visuals to the user's grasp. For all the rest of comparisons (from midair pinch to a rigid object), we found that the CapstanCrunch beats the spring device, especially for more rigid objects, where the spring performs particularly bad.

However, CapstanCrunch did not beat the levels of realistic rigidity accomplished by the CLAW. Despite the CapstanCrunch scores, results were nonetheless quite satisfactory on rigid devices. We hypothesize that future changes in the CapstanCrunch might include faster actuation to improve the rendering of rigid objects. With faster actuators, grasping rigid objects could feel stiffer where the onset of force and its release would occur over shorter times.

On the other hand, CapstanCrunch was much better than CLAW in rendering a midair grasp. The main issue with the CLAW was the background resistance force that is created by the particular choice of its motor and force sensor. The CLAW operates at a minimum resistance that is quite significant when compared to the zero resistance that CapstanCrunch can achieve when the brake does not engage. This is of course a design limitation and a better design could actuate CLAW at lower idle resistances. In contrast, our capstan design can perform better with less expensive actuators. Our mechanism was able to magnify the internal actuator's force by a factor of around 40. Compared to active force control devices, our approach is low cost, stable, low electrical power, robust, safe, fast and quiet, while providing high force control for user interaction.

The embedded resistance problem of CLAW also persisted for simulations of very small k (spring constant). Therefore, the CLAW performed at higher accuracies only for compliances over a certain k . These limitations to render very squishy objects from the CLAW, together with the limitations of the Spring device to render very rigid objects, made the CapstanCrunch appear the most preferred device when the scores were aggregated.

These results suggest that our unique design of a brake capstan + clutch succeeded at creating variable k for the grasping of objects. Interestingly, this was accomplished despite the k values for the CapstanCrunch were only modulated in one direction - towards the grip of the object, while the k values on the release were always fixed and independent of the rendered object. This limitation of the brake actuated system did not seem to bother users. In light of these results, we hypothesize that grasp is indeed a non-symmetric task and more similar to the grapping of other asymmetric-grasping animals such as lobster claws or crocodile mouths that are much stronger in the gripping than the releasing directions of the grasp.

This hypothesis is further validated by the fact that the CLAW, which is a symmetric device, did not show significant differences to our prototype in most of the renderings.

CONCLUSIONS AND FUTURE WORK

We presented CapstanCrunch, a haptic controller for rendering grasping feedback up to human-scale forces. CapstanCrunch is built around a novel adjustable friction-based capstan-plus-cord brake that magnifies the forces of the small internal actuator in our controller to sustain user input. The internal actuators themselves are small, making our integrated controller robust and strong, yet cheap, low-power, and lightweight unlike many previous known or postulated controllers. CapstanCrunch employs the same capstan principle to drive a spring, which can selectively render haptic compliance in response to grasping. CapstanCrunch is capable of providing a comprehensive set of compliant haptics enabled through a mechanism that is dynamically controlled by a small internal actuator.

In our evaluation, we compared CapstanCrunch with a previous active grasp feedback controller as well as a passive spring controller, showing participants' higher ratings for CapstanCrunch's rendered compliant haptic feedback over the two other devices.

We also evaluated CapstanCrunch's asymmetric spring constant k that applies forces only for the grasp direction but not for release, which was validated as a reasonable approach by participants during the user study. The results show the promising outlook for brake-operated controller devices that enable asymmetric compliance in agreement with the existence of a more fundamental asymmetry of grasp but will need to be further validated in the future.

Future work will also focus on reducing component sizes. We hope to shrink the capstan and actuator volumes and incorporating them within the palm grip handle (e.g., similar to [22]). This development would also aid in incorporating similar haptic mechanisms for more than one finger.

Finally, in order to add normal cutaneous touch of the object held in hand, we plan to install a voice coil actuator in the fingertip supporting. We will also add a trackpad on the thumb rest (e.g., similar to [28]) in order to add the ability for finer manipulation to the object once it is in hand [2].

REFERENCES

1. Parastoo Abtahi and Sean Follmer. 2018. Visuo-Haptic Illusions for Improving the Perceived Performance of Shape Displays. *Proceedings of the 2018 CHI Conference on Human Factors in Computing Systems*, ACM, 150:1--150:13. <http://doi.org/10.1145/3173574.3173724>
2. Michael J Adams, Simon A Johnson, Philippe Lefèvre, et al. 2013. Finger pad friction and its role in grip and touch. *Journal of The Royal Society Interface* 10, 80.
3. Priyanshu Agarwal and Ashish D Deshpande. 2017. Series elastic actuators for small-scale robotic

- applications. *Journal of Mechanisms and Robotics* 9, 3, 31016.
4. Tomohiro Amemiya and Taro Maeda. 2008. Asymmetric oscillation distorts the perceived heaviness of handheld objects. *IEEE Transactions on Haptics* 1, 1, 9–18.
 5. Jinung An and Dong-Soo Kwon. 2006. Stability and performance of haptic interfaces with active/passive actuators—theory and experiments. *The International Journal of Robotics Research* 25, 11, 1121–1136.
 6. Mahdi Azmandian, Mark Hancock, Hrvoje Benko, Eyal Ofek, and Andrew D Wilson. 2016. Haptic Retargeting: Dynamic Repurposing of Passive Haptics for Enhanced Virtual Reality Experiences. *Proceedings of the 2016 CHI Conference on Human Factors in Computing Systems*, ACM, 1968–1979.
 7. Hrvoje Benko, Christian Holz, Mike Sinclair, and Eyal Ofek. 2016. NormalTouch and TextureTouch: High-fidelity 3D Haptic Shape Rendering on Handheld Virtual Reality Controllers. *Proceedings of the 29th Annual Symposium on User Interface Software and Technology*, 717–728. <http://doi.org/10.1145/2984511.2984526>
 8. Christopher C Berger and Mar Gonzalez-Franco. 2018. Expanding the Sense of Touch Outside the Body. *Proceedings of the 15th ACM Symposium on Applied Perception*, ACM, 10:1--10:9. <http://doi.org/10.1145/3225153.3225172>
 9. Christopher C Berger, Mar Gonzalez-Franco, Eyal Ofek, and Ken Hinckley. 2018. The uncanny valley of haptics. *Science Robotics* 3, 17. <http://doi.org/10.1126/scirobotics.aar7010>
 10. Jonathan Blake and Hakan B Gurocak. 2009. Haptic glove with MR brakes for virtual reality. *IEEE/ASME Transactions On Mechatronics* 14, 5, 606–615.
 11. Mourad Bouzit, George Popescu, Grigore Burdea, and Rares Boian. 2002. The Rutgers Master II-ND Force Feedback Glove. *Proceedings of the 10th Symposium on Haptic Interfaces for Virtual Environment and Teleoperator Systems*, IEEE Computer Society, 145--.
 12. Stephen Brewster and Lorna M Brown. 2004. Tactons: structured tactile messages for non-visual information display. *Proceedings of the fifth conference on Australasian user interface-Volume 28*, Australian Computer Society, Inc., 15–23.
 13. Lung-Pan Cheng, Eyal Ofek, Christian Holz, Hrvoje Benko, and Andrew D Wilson. 2017. Sparse haptic proxy: Touch feedback in virtual environments using a general passive prop. *Proceedings of the 2017 CHI Conference on Human Factors in Computing Systems*, ACM, 3718–3728.
 14. Francesco Chinello, Claudio Pacchierotti, Monica Malvezzi, and Domenico Prattichizzo. 2018. A Three Revolute-Revolute-Spherical Wearable Fingertip Cutaneous Device for Stiffness Rendering. *IEEE Transactions on Haptics* 11, 1, 39–50. <http://doi.org/10.1109/TOH.2017.2755015>
 15. Inrak Choi, Heather Culbertson, Mark R. Miller, Alex Olwal, and Sean Follmer. 2017. Gravity: A Wearable Haptic Interface for Simulating Weight and Grasping in Virtual Reality. *Proceedings of the 30th Annual ACM Symposium on User Interface Software and Technology*, 119–130. <http://doi.org/10.1145/3126594.3126599>
 16. Inrak Choi, Elliot W Hawkes, David L Christensen, Christopher J Ploch, and Sean Follmer. 2016. Wolverine: A wearable haptic interface for grasping in virtual reality. *Intelligent Robots and Systems (IROS), 2016 IEEE/RSJ International Conference on*, 986–993.
 17. Inrak Choi, Eyal Ofek, Hrvoje Benko, Mike Sinclair, and Christian Holz. 2018. CLAW: A Multifunctional Handheld Haptic Controller for Grasping, Touching, and Triggering in Virtual Reality. *Proceedings of the 2018 CHI Conference on Human Factors in Computing Systems*, 654:1–654:13. <http://doi.org/10.1145/3173574.3174228>
 18. François Conti and Oussama Khatib. 2009. A new actuation approach for haptic interface design. *The International Journal of Robotics Research* 28, 6, 834–848.
 19. Mark R Cutkosky. 1989. On grasp choice, grasp models, and the design of hands for manufacturing tasks. *IEEE Transactions on robotics and automation* 5, 3, 269–279.
 20. Takahiro Endo, Haruhisa Kawasaki, Tetsuya Mouri, et al. 2011. Five-fingered haptic interface robot: HIRO III. *IEEE Transactions on Haptics* 4, 1, 14–27.
 21. N Falcon. 2014. “Novint falcon haptic device. *Novint Technologies*.
 22. Igor Gaponov, Dmitry Popov, and Jee-Hwan Ryu. 2014. Twisted string actuation systems: A study of the mathematical model and a comparison of twisted strings. *IEEE/ASME Transactions on Mechatronics* 19, 4, 1331–1342.
 23. Mar Gonzalez-Franco and Christopher C Berger. 2019. Avatar embodiment enhances haptic confidence on the out-of-body touch illusion. *IEEE transactions on haptics*.
 24. Mar Gonzalez-Franco, Christopher C Berger, and Ken Hinckley. 2018. If (Virtual) Reality Feels Almost Right, It’s Exactly Wrong. *Scientific American*.
 25. Mar Gonzalez-Franco and Jaron Lanier. 2017. *Model of Illusions and Virtual Reality*. <http://doi.org/10.3389/fpsyg.2017.01125>
 26. Xiaochi Gu, Yifei Zhang, Weize Sun, Yuanzhe Bian, Dao Zhou, and Per Ola Kristensson. 2016. Dexmo: An Inexpensive and Lightweight Mechanical Exoskeleton for Motion Capture and Force Feedback in VR.

- Proceedings of the 2016 CHI Conference on Human Factors in Computing Systems*, ACM, 1991–1995. <http://doi.org/10.1145/2858036.2858487>
27. Seongkook Heo, Christina Chung, Geehyuk Lee, and Daniel Wigdor. 2018. Thor's Hammer: An Ungrounded Force Feedback Device Utilizing Propeller-Induced Propulsive Force. *Proceedings of the 2018 CHI Conference on Human Factors in Computing Systems*, 525:1--525:11. <http://doi.org/10.1145/3173574.3174099>
 28. Jaeyeon Jaeyeon Lee, Mike Sinclair, Mar Gonzalez-Franco, Eyal Ofek, and Christian Holz. 2019. TORC: A Virtual Reality Controller for In-Hand High-Dexterity Finger Interaction. *Proceedings of the 2019 CHI Conference on Human Factors in Computing Systems*.
 29. SungKu Kang, HyunKi In, and Kyu-Jin Cho. 2012. Design of a passive brake mechanism for tendon driven devices. *International Journal of Precision Engineering and Manufacturing* 13, 8, 1487–1490.
 30. Rebecca P Khurshid, Naomi T Fitter, Elizabeth A Fedalei, and Katherine J Kuchenbecker. 2017. Effects of grip-force, contact, and acceleration feedback on a teleoperated pick-and-place task. *IEEE transactions on haptics* 10, 1, 40–53.
 31. CyberGlove Systems LLC. CyberGrasp. *CyberGlove Systems LLC*. Retrieved September 6, 2018 from <http://www.cyberglovesystems.com/cybergrasp/>
 32. Karon E MacLean, Michael J Shaver, and Dinesh K Pai. 2002. Handheld haptics: A usb media controller with force sensing. *Proceedings 10th Symposium on Haptic Interfaces for Virtual Environment and Teleoperator Systems. HAPTICS 2002*, IEEE, 311–318.
 33. Thomas H Massie and J Kenneth Salisbury. 1994. The phantom haptic interface: A device for probing virtual objects. *Proceedings of the ASME winter annual meeting, symposium on haptic interfaces for virtual environment and teleoperator systems*, Citeseer, 295–300.
 34. Kouta Minamizawa, Souichiro Fukamachi, Hiroyuki Kajimoto, Naoki Kawakami, and Susumu Tachi. 2007. Gravity Grabber: Wearable Haptic Display to Present Virtual Mass Sensation. *ACM SIGGRAPH 2007 Emerging Technologies*, ACM. <http://doi.org/10.1145/1278280.1278289>
 35. Jun Murayama, Laroussi Bougrila, YanLin Luo, et al. 2004. SPIDAR G&G: a two-handed haptic interface for bimanual VR interaction. *Proceedings of EuroHaptics*, Citeseer, 138–146.
 36. Martin Murer, Bernhard Maurer, Hermann Huber, Ilhan Aslan, and Manfred Tscheligi. 2015. Torquescreen: Actuated flywheels for ungrounded kinaesthetic feedback in handheld devices. *Proceedings of the Ninth International Conference on Tangible, Embedded, and Embodied Interaction*, ACM, 161–164.
 37. D. Prattichizzo, F. Chinello, C. Pacchierotti, and M. Malvezzi. 2013. Towards Wearability in Fingertip Haptics: A 3-DoF Wearable Device for Cutaneous Force Feedback. *IEEE Transactions on Haptics* 6, 4, 506–516. <http://doi.org/10.1109/TOH.2013.53>
 38. Domenico Prattichizzo, Francesco Chinello, Claudio Pacchierotti, and Monica Malvezzi. 2013. Towards Wearability in Fingertip Haptics: A 3-DoF Wearable Device for Cutaneous Force Feedback. *IEEE Transactions on Haptics* 6, 4, 506–516. <http://doi.org/10.1109/TOH.2013.53>
 39. Carlos Rossa, José Lozada, and Alain Micaelli. 2014. Design and control of a dual unidirectional brake hybrid actuation system for haptic devices. *IEEE transactions on haptics* 7, 4, 442–453.
 40. Timothy M Simon, Ross T Smith, and Bruce H Thomas. 2014. Wearable jamming mitten for virtual environment haptics. *Proceedings of the 2014 ACM International Symposium on Wearable Computers*, ACM, 67–70.
 41. Massimiliano Solazzi, Antonio Frisoli, and Massimo Bergamasco. 2010. Design of a cutaneous fingertip display for improving haptic exploration of virtual objects. *19th International Symposium in Robot and Human Interactive Communication*, IEEE, 1–6.
 42. Bernhard Spanlang, Jean-Marie Normand, David Borland, et al. 2014. How to Build an Embodiment Lab: Achieving Body Representation Illusions in Virtual Reality. *Frontiers in Robotics and AI* 1, November, 1–22. <http://doi.org/10.3389/frobt.2014.00009>
 43. Evan Strasnick, Christian Holz, Eyal Ofek, Mike Sinclair, and Hrvoje Benko. 2018. Haptic Links: Bimanual Haptics for Virtual Reality Using Variable Stiffness Actuation. *Proceedings of the 2018 CHI Conference on Human Factors in Computing Systems*, 644:1–644:12. <http://doi.org/10.1145/3173574.3174218>
 44. Colin Swindells, Alex Unden, and Tao Sang. 2003. TorqueBAR: an ungrounded haptic feedback device. *Proceedings of the 5th international conference on Multimodal interfaces*, ACM, 52–59.
 45. Dzmitry Tsetserukou, Shotaro Hosokawa, and Kazuhiko Terashima. 2014. LinkTouch: A wearable haptic device with five-bar linkage mechanism for presentation of two-DOF force feedback at the fingerpad. *2014 IEEE Haptics Symposium (HAPTICS)*, IEEE, 307–312.
 46. Bogdan Vigar, James Sulzer, and Roger Gassert. 2015. Design and evaluation of a cable-driven fMRI-compatible haptic interface to investigate precision grip control. *IEEE transactions on haptics* 9, 1, 20–32.
 47. Julie M Walker, Heather Culbertson, Michael Raitor, and Allison M Okamura. 2018. Haptic orientation guidance using two parallel double-gimbal control moment gyroscopes. *IEEE transactions on haptics* 11, 2, 267–

48. Eric Whitmire, Hrvoje Benko, Christian Holz, Eyal Ofek, and Mike Sinclair. 2018. Haptic Revolver: Touch, Shear, Texture, and Shape Rendering on a Reconfigurable Virtual Reality Controller. *Proceedings of the 2018 CHI Conference on Human Factors in Computing Systems*, 86:1–86:12. <http://doi.org/10.1145/3173574.3173660>
49. Andre Zenner, Antonio Kruger, A. Krüger, Antonio Kruger, and A. Krüger. 2017. Shifty: A Weight-Shifting Dynamic Passive Haptic Proxy to Enhance Object Perception in Virtual Reality. *IEEE Transactions on Visualization and Computer Graphics* 23, 4, 1285–1294. <http://doi.org/10.1109/TVCG.2017.2656978>
50. Yuhang Zhao, Cynthia L Bennett, Hrvoje Benko, et al. 2018. Enabling People with Visual Impairments to Navigate Virtual Reality with a Haptic and Auditory Cane Simulation. *Proceedings of the 2018 CHI Conference on Human Factors in Computing Systems*, ACM, 116:1--116:14. <http://doi.org/10.1145/3173574.3173690>
51. Igor Zubrycki and Grzegorz Granosik. 2017. Novel haptic device using jamming principle for providing kinaesthetic feedback in glove-based control interface. *Journal of Intelligent & Robotic Systems* 85, 3–4, 413–429.
52. 2018. DextrES: Wearable Haptic Feedback for Grasping in VR via a Thin Form-Factor Electrostatic Brake. ACM.